

AD-A052 721

AIR FORCE INST OF TECH WRIGHT-PATTERSON AFB OHIO
AN ATOMIC FLUORESCENCE SYSTEM USING A CONTINUUM SOURCE FOR THE --ETC(U)
MAR 78 R L VAUGHN
AFIT-CI-78-53

F/G 7/4

UNCLASSIFIED

NL

| OF |
AD
A052 721



END
DATE
FILMED
5-78
DDC

AD A 052721

AD No.
DDC FILE COPY

AN ATOMIC FLUORESCENCE SYSTEM USING A CONTINUUM SOURCE
FOR THE RAPID DETERMINATION OF WEAR METALS
IN JET ENGINE LUBRICATING OILS

By

ROBERT L. VAUGHN



A THESIS PRESENTED TO THE GRADUATE COUNCIL OF
THE UNIVERSITY OF FLORIDA
IN PARTIAL FULFILLMENT OF THE REQUIREMENTS FOR THE
DEGREE OF MASTER OF SCIENCE

UNIVERSITY OF FLORIDA

1978

This document has been approved
for public release and sale; its
distribution is unlimited.

UNCLASSIFIED

SECURITY CLASSIFICATION OF THIS PAGE (When Data Entered)

REPORT DOCUMENTATION PAGE		READ INSTRUCTIONS BEFORE COMPLETING FORM
1. REPORT NUMBER CI-78-53	2. GOVT ACCESSION NO.	3. RECIPIENT'S CATALOG NUMBER (9)
4. TITLE (and Subtitle) An Atomic Fluorescence System Using a Continuum Source for the Rapid Determination of Wear Metals in Jet Engine Lubricating Oils.		5. TYPE OF REPORT & PERIOD COVERED Master's Thesis
7. AUTHOR(s) Captain Robert L. Vaughn		6. PERFORMING ORG. REPORT NUMBER
9. PERFORMING ORGANIZATION NAME AND ADDRESS AFIT Student at the University of Florida Gainesville FL		8. CONTRACT OR GRANT NUMBER(s)
11. CONTROLLING OFFICE NAME AND ADDRESS AFIT/CI WPAFB OH 45433 (12) 65p.		10. PROGRAM ELEMENT, PROJECT, TASK AREA & WORK UNIT NUMBERS (11) May 78
14. MONITORING AGENCY NAME & ADDRESS (if different from Controlling Office)		12. REPORT DATE 1978
		13. NUMBER OF PAGES 57 Pages
		15. SECURITY CLASS. (of this report) Unclassified
16. DISTRIBUTION STATEMENT (of this Report) Approved for Public Release; Distribution Unlimited		15a. DECLASSIFICATION/DOWNGRADING SCHEDULE
17. DISTRIBUTION STATEMENT (of the abstract entered in Block 20, if different from Report)		
18. SUPPLEMENTARY NOTES JERRAL F. GUESS, Captain, USAF Director of Information, AFIT APPROVED FOR PUBLIC RELEASE AFR 190-17.		
19. KEY WORDS (Continue on reverse side if necessary and identify by block number)		
20. ABSTRACT (Continue on reverse side if necessary and identify by block number)		

DD FORM 1 JAN 73 1473

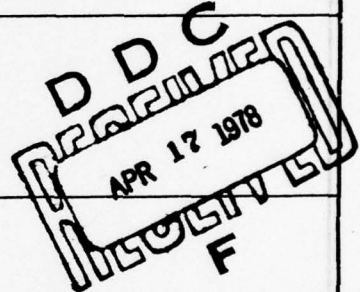
EDITION OF 1 NOV 65 IS OBSOLETE

UNCLASSIFIED

SECURITY CLASSIFICATION OF THIS PAGE (When Data Entered)

012 200

1B



AN ATOMIC FLUORESCENCE SYSTEM USING A CONTINUUM SOURCE
FOR THE RAPID DETERMINATION OF WEAR METALS
IN JET ENGINE LUBRICATING OILS

By

ROBERT L. VAUGHN

A THESIS PRESENTED TO THE GRADUATE COUNCIL OF
THE UNIVERSITY OF FLORIDA
IN PARTIAL FULFILLMENT OF THE REQUIREMENTS FOR THE
DEGREE OF MASTER OF SCIENCE

UNIVERSITY OF FLORIDA

1978

ACKNOWLEDGEMENTS

The author thanks Dr. J.D. Winefordner for the opportunity to work with his research group. He also appreciates the assistance of Drs. M. Vala and R.G. Bates.

The author is especially grateful to John Bradshaw for the time and effort he so willingly gave. He was always available for advice and help.

Finally, the author thanks Jo Anne, his wife, for her patience and understanding when it was needed most.

Administrative for	
File Section	<input checked="" type="checkbox"/>
Ext. Section	<input type="checkbox"/>
Distribution/Availability Codes	
AD	SPECIAL
A	

TABLE OF CONTENTS

	<u>Page</u>
ACKNOWLEDGEMENTS.	ii
ABSTRACT.	iv
INTRODUCTION.	1
THEORY.	6
EXPERIMENTAL.	20
RESULTS	28
DISCUSSION.	35
CONCLUSIONS	42
APPENDICES	
A CURRENT CONTROL/TIMING CIRCUIT	43
B TEMPERATURE CALIBRATION DATA	50
C SLIT WIDTH AND ARGON FLOW OPTIMIZATION	52
LIST OF REFERENCES.	54
BIOGRAPHICAL SKETCH	57

Abstract of Thesis Presented to the Graduate Council
of the University of Florida in Partial Fulfillment of the
Requirements for the Degree of Master of Science

AN ATOMIC FLUORESCENCE SYSTEM USING A CONTINUUM SOURCE
FOR THE RAPID DETERMINATION OF WEAR METALS
IN JET ENGINE LUBRICATING OILS

By

Robert L. Vaughn

March, 1978

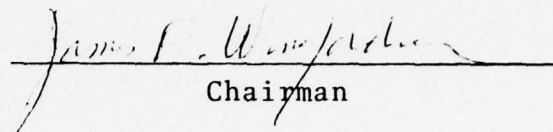
Chairman: James D. Winefordner
Major Department: Chemistry

A brief review is presented of atomic absorption and atomic fluorescence methods of trace wear-metal analysis of jet engine lubricating oil. The theory of atomic fluorescence in flames is presented for the case of a continuum excitation source.

A system for atomic fluorescence measurements is described that employs an electrically-heated graphite rod and a N_2O/C_2H_2 flame atomizer with a 300-W Eimac xenon arc as the continuum excitation source. With this system, small samples (1 ^{microliter} ~~μl~~) having complex matrices can be analyzed rapidly, conveniently, and with no pretreatment.

Analytical calibration curves are given for Cr, Al, and Mo, and these metals are determined in synthetic and real jet engine lubricating oils. The determinations of these elements are evaluated with respect to the accuracy and repeatability criteria of the Interservice Oil Analysis Program.

Sources of errors associated with sampling, interferences, and the graphite rod are discussed.


Chairman

INTRODUCTION

Application of trace element analysis to the determination of wear metal particles suspended in lubricating oils of railroad and aircraft engines has been used for many years. The first-used methods of analysis included colorimetry and a number of direct atomic emission spectrographic techniques. Atomic absorption spectroscopy (AAS) emerged in the 1960's as the primary method of analysis of trace wear metals in lubricating oils (1). *AC used and A A*

In 1964, atomic fluorescence spectroscopy (AFS) was developed as an analytical technique by Winefordner and Vickers (2) and Winefordner and Staab (3). Atomic fluorescence spectroscopy was slightly later used by West (4) and Dagnall, West, and Young (5).

Atomic fluorescence spectroscopy has a number of advantages over AAS. Atomic fluorescence spectroscopy is especially valuable for determinations of very low concentrations of certain elements, and through the use of a continuum source, for rapid, multielement determinations. In addition, the linear working concentration range for AFS is about ten times that of AAS (6).

The first commercial atomic fluorescence spectrometer, based on the design of Mitchell and Johansson (7) in 1970,

consisted of six sequentially pulsed hollow cathode lamps. The instrument was marketed for only a short time, and presently, there is no AFS system commercially available.

Preliminary investigations of AFS for wear-metal analysis in lubricating oils were made by Smith, Stafford, and Winefordner (8) and Miller, Fraser, and Winefordner (9). Smith et al. used electrodeless discharge tubes as spectral sources and total-consumption burners supporting hydrogen-argon-entrained-air or hydrogen-air flames. They obtained satisfactory results for Ag, Cu, Fe, Mg, Ni, and Pb, but not for Al, Cr, Sn, or Ti. No pretreatment of the oil samples was required. Using the premixed hydrogen-air flame, the authors performed a ten-fold dilution of the oil samples with methyl isobutyl ketone.

Miller et al. used a 150-W Eimac xenon arc continuum source and a total-consumption nebulizer-burner with a hydrogen-argon-entrained-air flame. The oil samples were diluted four-fold with carbon tetrachloride. Good results were obtained for Fe, Cu, Ag, and Mg.

Although spectral continuum sources generally give poorer detection limits than intense line sources, they have the advantages of being more stable, more reproducible from day to day, and have longer life. More importantly, one source can be used to excite all elements (10).

Johnson, Plankey, and Winefordner (11) tried both a pulsed xenon lamp and a cw xenon arc point source with a special mirror enabling the transfer of nearly all the

radiation to the absorption cell. For both source types, they studied good atomizing flames (argon-separated air/C₂H₂ or N₂O/C₂H₂). They reported analytical figures of merit for Ag, Cd, Co, Cr, Mg, Mn, Se, and Zn using the air/C₂H₂ flame and for Al, Be, Ti, Mo, and V using the N₂O/C₂H₂ flame. They also determined Fe, Mg, Cu, Ag, and Cr in used jet engine lubricating oils. The same authors (12) demonstrated the utility of the continuum source for determining wear metals in oil. They obtained analytical data for Ag, Cr, Cu, Fe, Mg, Ni, and Pb without sample dilution.

Johnson, Plankey, and Winefordner (13) refined their technique (11, 12) by the addition of a computer-controlled, slewed-scan spectrometer. They obtained detection limits and analytical calibration curves for 18 elements in aqueous samples (Ag, Au, Cd, Cr, Co, Cu, Fe, In, Mg, Mn, Ni, Pb, Pd, Pt, Sn, Sr, Tl, and Zn) with the air/C₂H₂ flame and 5 elements (Al, Be, Mo, Ti, and V) with the N₂O/C₂H₂ flame. They determined 5 elements in lubricating oils (Fe, Mg, Cu, Ag, and Cr).

In 1972, Molnar et al. (14) described a simple, electrically-heated graphite rod atomizer with a hydrogen-argon-entrained-air flame around and above the rod for atomic absorption studies. Measurements were made for Ag, As, Au, Cr, Cu, Fe, Mg, Ni, and Pb in aqueous samples and for Ag, Cu, and Fe in jet engine lubricating oil samples diluted ten-fold with isooctane. Reeves et al. (15) used the same atomizer

for atomic absorption determinations for Ag, Cr, Cu, Fe, Ni, Pb, and Sn in jet engine lubricating oils.

Other workers also investigated furnace atomizers for trace metal analysis of oil-based samples. Brodie and Matousek (16) used a graphite mini-Massmann furnace to determine Ag, Al, Cu, Cr, Mg, Ni, and Pb in 1- μ l undiluted oil samples. Alder and West (17) used a graphite rod atomizer for Ag and Cu in diesel engine oil. Omang (18) determined Ni and V in crude petroleum in a graphite tube furnace. Reeves, Molnar, and Winefordner (19) sequentially atomized Ag and Cu from a graphite rod with a multielement hollow cathode lamp spectral source for atomic absorption measurements.

Patel et al. (20) used the graphite rod atomizer described by Molnar et al. (14) for atomic fluorescence studies. Using electrodeless discharge lamps as sources, they determined Ag, Cd, Cu, Hg, Pb, Sn, Tl, and Zn in aqueous samples and Ag, Pb, and Sn in oil-based samples.

More recently, Katskov, Kruglikova, and L'vov (21) reported using an electrically heated graphite chamber in an air/C₂H₂ or N₂O/C₂H₂ flame. They made atomic absorption determinations on 27 elements, including Ti, V, Mo, and Si in ores, rocks, slags, metals, refractory-metal oxides, biological materials, paper, and oils. The same chamber was used by Razumov (22), combined with a natural gas flame, for both atomic absorption and atomic fluorescence studies.

This study employed a graphite rod furnace essentially the same as described by Molnar et al. (14), except that it was modified with a circular burner to support an argon-sheathed N_2O/C_2H_2 flame. The graphite rod allowed the direct introduction of small-sized samples having complex matrices, eliminating the need for dilution or other pretreatment of the sample. This graphite rod-flame atomizer, when combined with a continuum source for AFS, provided an operationally-simple, sensitive system for multielement trace analysis for the elements Cr, Al, and Mo in samples having complex matrices.

THEORY

Although the furnace used in this work incorporated a graphite rod, the experimental data were interpreted on the basis of flame theory since the absorption was performed within the flame region assumed to be in thermodynamic equilibrium (23, 24).

The sample cell was assumed to be a parallelepiped (see Figure 1) with absorption path length ℓ cm, luminescence path length L cm, and height ℓ' cm. A cylindrical cell is more difficult to treat exactly; however, a cylindrical cell of radius r results in about the same luminescence radiance as a parallelepiped with a square cross section of ℓ^2 where ℓ is related to r by $\ell = r \sqrt{\pi}$. It was assumed that the analyte absorbers were equally and uniformly distributed within the cell and that no interferences were present, that is, that only the analyte absorbed and that only the analyte luminesced. Because fluorescence was being measured perpendicular to the excitation beam, it was also assumed that all the luminescence from the face of area $\ell\ell'$ was measured and that the entire front surface of area $L\ell'$ was fully illuminated, that is, that there were no prefilter and postfilter effects.

If the spectral radiance of a continuum source is $B_{S\lambda 0}$ ($\text{erg s}^{-1} \text{ cm}^{-2} \text{ sr}^{-1} \text{ nm}^{-1}$) at the excitation wavelength λ , then

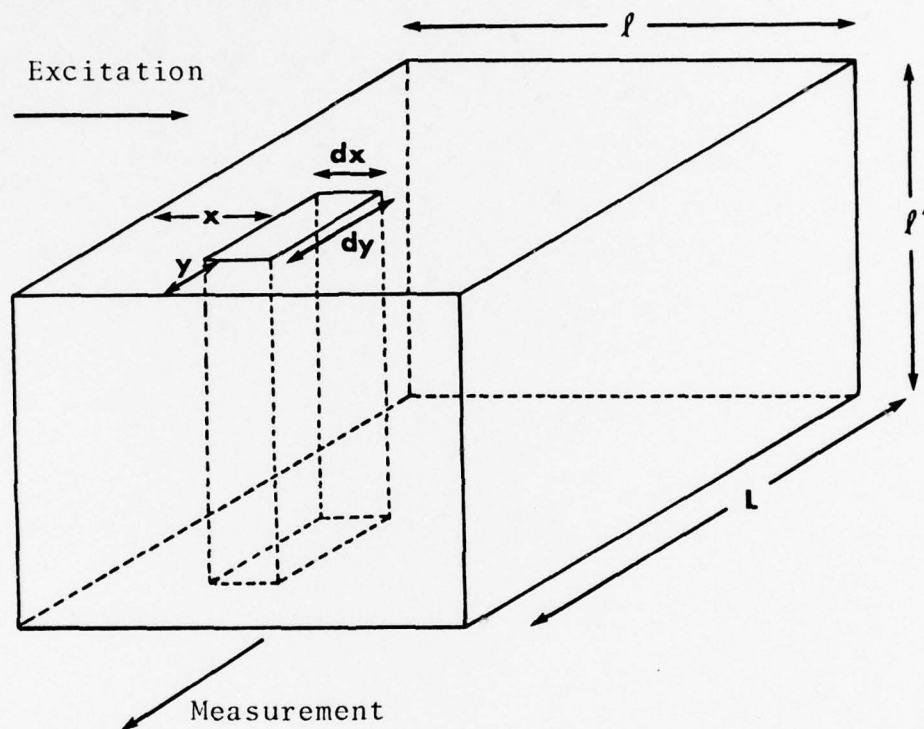


Figure 1. Schematic diagram of cell assumed for luminescence radiance expressions, showing dimensions of unit cell (25).

the source spectral radiance flux $\phi_{S\lambda 0}$ ($\text{erg s}^{-1} \text{ nm}^{-1}$) incident upon the cross-sectional area of $dy\lambda'$ cm^2 of the volume element $dydx\lambda'$ cm^3 is

$$\phi_{S\lambda 0} = B_{S\lambda 0} \Omega_E [dy\lambda'] \left(\frac{1}{m_L m_H} \right) T_E \quad (1)$$

where Ω_E is the solid angle (sr) of exciting radiation collected by the entrance optics and imaged upon the volume element $dydx\lambda'$; m_L and m_H are source image magnification (dimensionless) at the cell surface in the longitudinal and the horizontal directions; T_E is a factor (dimensionless) to account for absorption and reflection losses due to optical components between the source and the absorption cell. The quantities Ω_E , m_L , m_H , and T_E are assumed to be independent of excitation wavelength, which is a reasonable approximation for mirrors or lenses not used near their absorption cutoff wavelengths, assuming the wavelength range is not too large (less than about 1000 Å).

Then, from the Beer-Lambert absorption law, the spectral radiant flux at any distance x from the front surface of the cell, $\phi_{S\lambda}(x)$ ($\text{erg s}^{-1} \text{ nm}^{-1}$) is given by

$$\phi_{S\lambda}(x) = \phi_{S\lambda 0} [\exp(-k_\lambda x)] \quad (2)$$

where k_λ is the absorption coefficient (cm^{-1}) of the analyte at the excitation wavelength λ (i.e., the fraction absorbed).

The radiant flux absorbed at wavelength per unit wavelength interval by the small volume element of path length

dx is then given by

$$d\Phi_{S\lambda} = \Phi_{S\lambda 0} k_{\lambda} [\exp -k_{\lambda} x] dx \quad (3)$$

To convert radiant flux absorbed by the volume element $dx dy dz'$ to radiant flux luminesced, it is necessary to use $Y_{\lambda}(\lambda')$, the luminescence spectral power efficiency (dimensionless), which is given by

$$Y_{\lambda}(\lambda') = Y_p f(\lambda')$$

where Y_p is the power yield of luminescence (i.e., the luminescence radiant flux divided by the absorbed radiant flux and is dependent on the excitation wavelength λ for gaseous atoms and diatomic molecules with widely separated vibrational levels; $f(\lambda')$ is the spectral distribution of luminescence (dimensionless) and is dependent only on the luminescence wavelength λ' . The product $f(\lambda') d\lambda'$ represents the probability that an emitted photon has a wavelength between λ' and $\lambda' + d\lambda'$, that is, $\int_0^{\infty} f(\lambda') d\lambda' = 1$. Therefore, $f(\lambda')$ represents the normalized shape of the luminescence line or band and is given by

$$f(\lambda') = \frac{k_{\lambda'}}{\int_0^{\infty} k_{\lambda'} d\lambda'}$$

where $k_{\lambda'}$ is the absorption coefficient (cm^{-1}) for the luminescence wavelength λ' .

The luminescence spectral radiant flux $d\phi_{L\lambda}$, from the small volume element $dx dy \ell'$ is the product of the flux absorbed, the luminescence spectral power efficiency, and a factor to account for loss of luminescence due to self-absorption, and so

$$d\phi_{L\lambda} = d\phi_{S\lambda} Y_{\lambda}(\lambda') [\exp -k_{\lambda} y] dy \quad (4)$$

The spectral radiant flux of luminescence can be converted to the spectral radiance of luminescence by dividing $d\phi_{L\lambda}$, by 4π (there are 4π sr in a sphere of isotropic luminescence), by the area dA_S of the six surfaces of the volume element, and by n^2 , where n is the refractive index of the flame environment, and so

$$dB_{L\lambda} = d\phi_{L\lambda} \left(\frac{1}{4\pi n^2} \right) \left(\frac{1}{dA_S} \right) \quad (5)$$

For a gas such as a flame, $n \approx 1$.

The luminescence radiance dB_L ($\text{erg s}^{-1} \text{ cm}^{-2} \text{ sr}^{-1}$) from the volume element $dx dy \ell'$ is therefore given by

$$dB_L = \left[\frac{\Omega_E}{4\pi} \right] \left[\frac{\ell' dx dy}{dA_S} \right] \left[\frac{T_E}{n^2 m_L m_H} \right] \left[\frac{1}{\int_0^{\infty} k_{\lambda} d\lambda'} \right] \quad (6)$$

$$\cdot \left[\int_0^{\infty} \phi_{S\lambda} k_{\lambda} [\exp -k_{\lambda} x] d\lambda \right] \left[\int_0^{\infty} Y_p k_{\lambda} [\exp -k_{\lambda} y] d\lambda' \right]$$

If this equation is integrated with respect to x and y between the limits 0 and ℓ for x and 0 and L for y , then the

luminescence radiance B_L is given by

$$B_L = \left[\frac{\Omega_E}{4\pi} \right] \left[\frac{L\ell'}{2L\ell' + 2\ell\ell' + 2L\ell} \right] \left[\frac{T_E}{n^2 m_L m_H} \right] Y_p \cdot \left[\int_0^\infty B_{S\lambda} (1 - \exp -k_\lambda \ell) d\lambda \right] \left[\frac{\int_0^\infty (1 - \exp -k_{\lambda,L}) d\lambda'}{\int_0^\infty L k_{\lambda'} d\lambda'} \right] \quad (7)$$

This relationship is specifically the total line luminescence radiance, B_L , for the right angle case of continuum source illumination-measurement.

The first integral in Equation (7) is the absorbed radiance. The integral ratio on the far right is the self-absorption factor, f_s , and accounts for the reabsorption of luminescence by analyte species. The ratio f_s is unity or nearly unity for the case of atomic fluorescence involving a dilute atomic gas and transitions terminating in the ground state. However, for atomic fluorescence of concentrated ($k_{\lambda,y} \gg 1$ for λ 's near λ'_0) gases, the selfabsorption factor is less than unity and is given by

$$f_s = \frac{\int_0^\infty (1 - \exp -k'_{\lambda}, z) d\lambda'}{\int_0^\infty z k'_{\lambda}, d\lambda'} = \frac{2\sqrt{a'}}{\sqrt{(\sqrt{\pi} k'_0 z)}} \quad (8)$$

where $z = L$ for the right angle case and k_0 is the peak atomic absorption coefficient for pure Doppler broadening for the fluorescence line, and a' is the damping constant (dimension-

less) (accounts for collisional as well as Doppler broadening) for the fluorescence line and is given by

$$a' = \sqrt{\ln 2} \frac{\Delta\lambda_C'}{\Delta\lambda_D'}$$

where $\Delta\lambda_C'$ is the collisional half width (nm) of the fluorescence line and $\Delta\lambda_D'$ is the Doppler half width (nm) of the fluorescence line.

The first integral in Equation (7) is more difficult to evaluate because of the two wavelength-dependent terms, $B_{S\lambda_0}$ and $(1 - \exp -k_\lambda \ell)$. For atomic fluorescence being excited with a continuum source (source having a constant spectral radiance over the entire absorption line or band) the integral becomes

$$\int_0^\infty B_{S\lambda_0} (1 - \exp -k_\lambda \ell) d\lambda = B_{C\lambda_0}^0 \int_0^\infty (1 - \exp -k_\lambda \ell) d\lambda \quad (9)$$

where $B_{C\lambda_0}^0$ is the spectral radiance of the continuum source at the peak absorption wavelength. The integral in Equation (9) is readily solved for absorption lines or bands having a Voigt profile and resulting from either very low or very high concentration of absorbers. A spectral line or band with a Voigt profile (a line or band broadened by both Lorentzian and Gaussian effects) has an absorption coefficient of

$$k_{\lambda} = \frac{a}{\pi} k_0 \int_{-\infty}^{+\infty} \frac{\exp(-y^2) dy}{a^2 + (v - y)^2}$$

where a is the damping constant (dimensionless) and is given by $\sqrt{\ln 2}$ times the ratio of the Lorentzian half width to the Gaussian half width of the line or band, k_0 is the peak absorption coefficient (cm^{-1}) for pure Gaussian broadening (for atoms, Doppler broadening) for the excitation process, v is the relative wavelength (dimensionless) of any point in the absorption line in terms of Doppler half width, and y is a variable relative wavelength (dimensionless) taken with respect to v .

$$a = \sqrt{\ln 2} \frac{\Delta\lambda_C}{\Delta\lambda_D}$$

$$v = 2\sqrt{\ln 2} \frac{(\lambda - \lambda_0)}{\Delta\lambda_D}$$

$$y = 2\sqrt{\ln 2} \frac{\delta}{\Delta\lambda_D}$$

In the above relationships, $\Delta\lambda_C$ is the collisional half width (nm), $\Delta\lambda_D$ is the Doppler half width (nm), λ is any wavelength (nm), λ_0 is the peak wavelength, and δ is a variable distance from $\lambda - \lambda_0$ (nm).

The integral in Equation (9) is called the total absorption and given the symbol A_t . It can be evaluated for two limiting cases. For a low concentration ($k_0 \leq 0.05$) of absorbers,

$$\int_0^{\infty} (1 - \exp -k_{\lambda} \ell) d\lambda = \int_0^{\infty} k_{\lambda} \ell d\lambda = \frac{\sqrt{\pi} k_0 \Delta\lambda_D \ell}{2\sqrt{\ln 2}} \quad (10)$$

and for high concentration ($k_0 \ell \gg 10$) of absorbers

$$\int_0^{\infty} (1 - \exp -k_{\lambda} \ell) d\lambda = \Delta\lambda_D \sqrt{\left(\frac{\sqrt{\pi} k_0 \ell a}{\ln 2} \right)} \quad (11)$$

Combining Equations (7), (9), (10), and noting that f_s is about equal to unity, gives the radiance expression for a continuum source using right angle measurement and for a low concentration of analyte.

$$B_L = \left[\frac{\Omega_E}{4\pi} \right] \left[\frac{L \ell \ell'}{2L \ell' + 2\ell \ell' + 2L \ell} \right] \left[\frac{T_E}{n^2 m_L m_H} \right] \\ \cdot Y_L B_{C\lambda_0}^0 \left[\frac{\sqrt{\pi} k_0 \Delta\lambda_D}{2\sqrt{\ln 2}} \right]$$

For high concentration of analyte for atomic fluorescence terminating in the ground or near ground state and a continuum source, Equations (7), (8), (9), and (11) result in

$$B_L = \left[\frac{\Omega_E}{4\pi} \right] \left[\frac{L \ell'}{2L \ell' + 2\ell \ell' + 2L \ell} \right] \left[\frac{T_E}{n^2 m_L m_H} \right] \\ \cdot Y_L B_{C\lambda_0}^0 \left(\frac{k_0 \ell a a'}{k'_0 L \ln 2} \right)^{1/2} \Delta\lambda_D$$

From these relationships, some generalizations can be made for B_L . The luminescence radiance, B_L , is directly

proportional to the absorption coefficient, k_o , and thus to the concentration of analyte as long as the concentration of analyte, n_o , is low because k_o , the maximum absorption coefficient, is directly proportional to n_o , the concentration of analyte in the lower state,

$$k_o = \frac{2\sqrt{\ln 2} \lambda_o^4 n_o A_{u,1}}{8\pi\sqrt{\pi} c \Delta\lambda_D}$$

where λ_o is the peak absorption wavelength (cm), n_o is the concentration of analyte in the lower state involved in the absorption transition (cm^{-3}), $A_{u,1}$ is the Einstein coefficient of spontaneous emission (s^{-1}), c is the speed of light (cm s^{-1}), and $\Delta\lambda_D$ is the Doppler half width of the atomic line (cm).

Also, B_L is dependent only on the cell volume and not the cell shape as long as the concentration of absorbers is low, and as long as the entire cell cross-section of $L\ell' \text{ cm}^2$ is fully illuminated and the entire luminescence from the right hand face of $\ell\ell' \text{ cm}^2$ is measured. The luminescence radiance depends directly on the spectral radiance of the continuum source and directly on the luminescence power efficiency. Finally, B_L is independent of the spectral profiles of the absorption and luminescence bands as long as the absorber concentration is low and as long as a continuum source is used.

For any given atom, line, and flame, the quantities a , Y , $\Delta\lambda_D$, L , and ℓ are constant, and for any given source, $B_{C\lambda_o}$

is constant. Thus, for low concentrations,

$$B_L = \text{constant} \times k_o = \text{constant} \times n_o.$$

The concentration, n_o , of atoms in the lower state involved in the absorption process is determined by the Boltzmann distribution equation and is given by

$$n_o = n_t \frac{g_o}{Z_T} \exp \frac{-E_i}{kT}$$

where g_o is the statistical weight of the lower level (usually ground state), n_t is the total concentration of atoms in all states, E_i is the excitation energy (erg), T is the temperature of the system ($^{\circ}\text{K}$), and Z_T is the electronic partition function given by

$$Z_T = \sum_i g_i \exp \frac{-E_i}{kT}$$

where g_i is the statistical weight of state i , and E_i is the excitation energy of state i . If $E_i \gtrsim 0.5 \text{ eV}$ for the lowest lying excited state and if $T \gtrsim 3000^{\circ}\text{K}$, then $n_o \gtrsim n_t$ within 5%. For atoms with many levels (e.g., transition metals, rare earths), $n_o < n_t$.

The basic expression relating n_o (ground state atoms cm^{-3}) to analyte concentration, C_o (moles cm^{-3}), is given by

$$n_o = (6 \times 10^{23}) \frac{F \epsilon \beta C_o g_o}{Q_t e_f Z_T}$$

where F is the solution transport rate ($\text{cm}^3 \text{s}^{-1}$), Q_t is the flow rate of unburnt gases into the flame ($\text{cm}^3 \text{s}^{-1}$), e_f (dimensionless) is the expansion factor of flame gases relative to room temperature, and $\epsilon\beta$ is the efficiency (dimensionless) of producing atoms from the sample. In flames, $\epsilon\beta$ is often many times less than unity, but it should be near unity for substances that are completely vaporized from a cuvette.

If the sample is vaporized in a cuvette (cylindrical cell with an open end), the peak atomic concentration of analyte is given by

$$n_o = (6 \times 10^{23}) \frac{m_a \epsilon\beta g_o}{e_g V_c M_a Z_T}$$

where V_c is cuvette volume (cm^3), m_a is analyte mass (g), M_a is the atomic weight (amu) of the analyte, and e_g is the gas expansion factor (dimensionless) between the heated gas temperature and room temperature.

If the sample is vaporized from a heated filament into a continuous flowing stream of inert gas, and if the analyte mass is vaporized as a plug in time t , then the peak concentration, n_p , is given by

$$n_p = (6 \times 10^{23}) \frac{m_a \epsilon\beta g_o}{t e_g Q_a M_a Z_T}$$

where Q_a is the flow rate of the inert gas ($\text{cm}^3 \text{s}^{-1}$) past the filament.

Actually, the analyte concentration will vary with time. The time-dependent concentration, $n_{(t)}$, is a complex function of the amount of analyte on the filament, the type of filament, the area of coverage, the diffusion rate of analyte, the filament temperature, and other factors.

Growth curves consist of plots of the logarithm of the luminescence radiance, B_L (or a function of B_L), versus the logarithm of the concentration of absorbers, n_0 . The shape of the growth curves is the major factor in determining the shape of the analytical calibration curves (plots of the logarithm of instrumental signal due to luminescence, S_L , versus the logarithm of the concentration, C_0 , of the analyte placed in the measurement cell). Analytical calibration curve plots of $\log S_L$ versus $\log C_0$ should have the same slope as the growth curve plots of $\log B_L$ versus $\log n_0$ as long as S_L is linear with B_L and n_0 is linear with C_0 . The instrumental signal should be linear with B_L over a large range of radiances, and the concentration of absorbers should be linear with respect to C_0 over a wide concentration range. Typical atomic fluorescence growth curves for a continuum source assuming right angle measurement are shown in Figure 2.

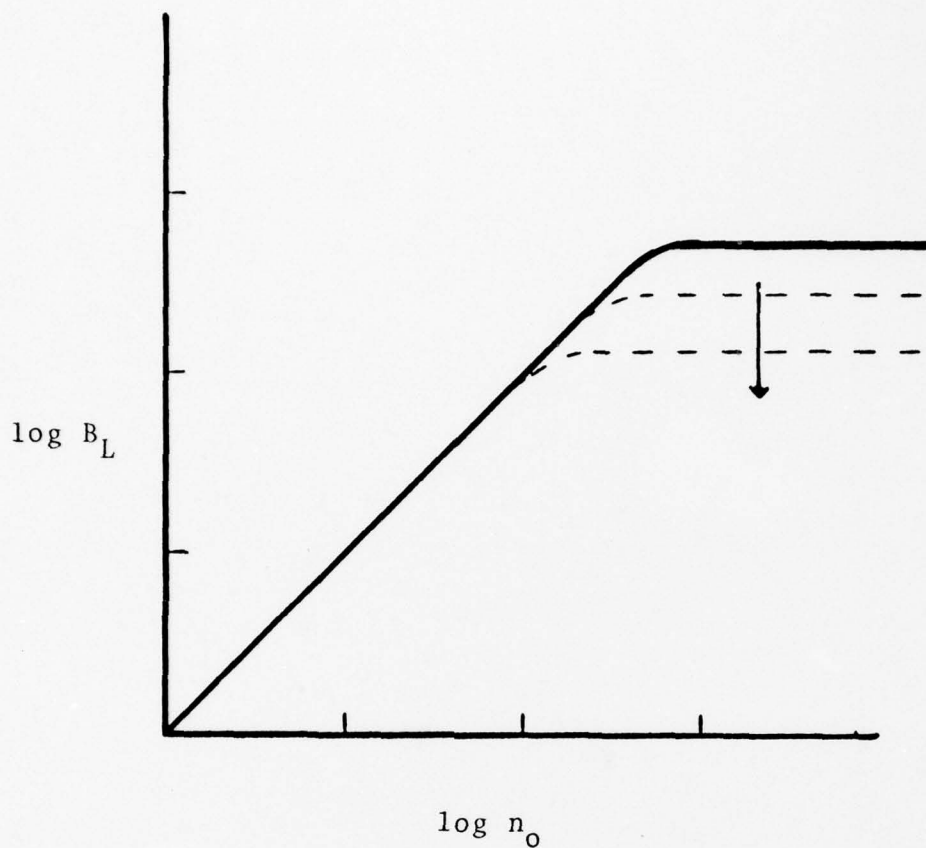


Figure 2. Atomic fluorescence growth curves for atoms excited by a continuum source and assuming right angle measurement. The dashed lines and arrow indicate the result of increasing prefilter and/or postfilter effects (26).

EXPERIMENTAL

Experimental System

A schematic of the experimental system is shown in Figure 3.

The excitation source was a 300-W Eimac xenon arc lamp (Varian Associates, Eimac Division, San Carlos, CA 94070). The Eimac lamp is a prefocused point source with a parabolical reflector that is highly efficient in producing atomic fluorescence for elements having resonance spectral lines with wavelengths longer than 200 nm (27).

The mirror and lenses L_1 and L_2 were set at the distances indicated in Figure 3 to focus the excitation beam to a spot 4 mm in diameter.

The atomizer (see Figure 4) consisted of a cylindrical bakelite block 8.2 cm in diameter and 2.6 cm high with water-cooled, copper blocks on either side to support a graphite rod and provide electrical contact with the power supply (SCR Power Supply, Electronic Measurements, Inc., model 10-250, Oceanport, NJ 07757).

A standard spectrographic-grade graphite rod (POCO Spectrographic Electrode, grade FXI, POCO Graphite, Inc., Decatur, TX 76234) was held firmly in place by small brass plates screwed into the tops of the copper blocks.

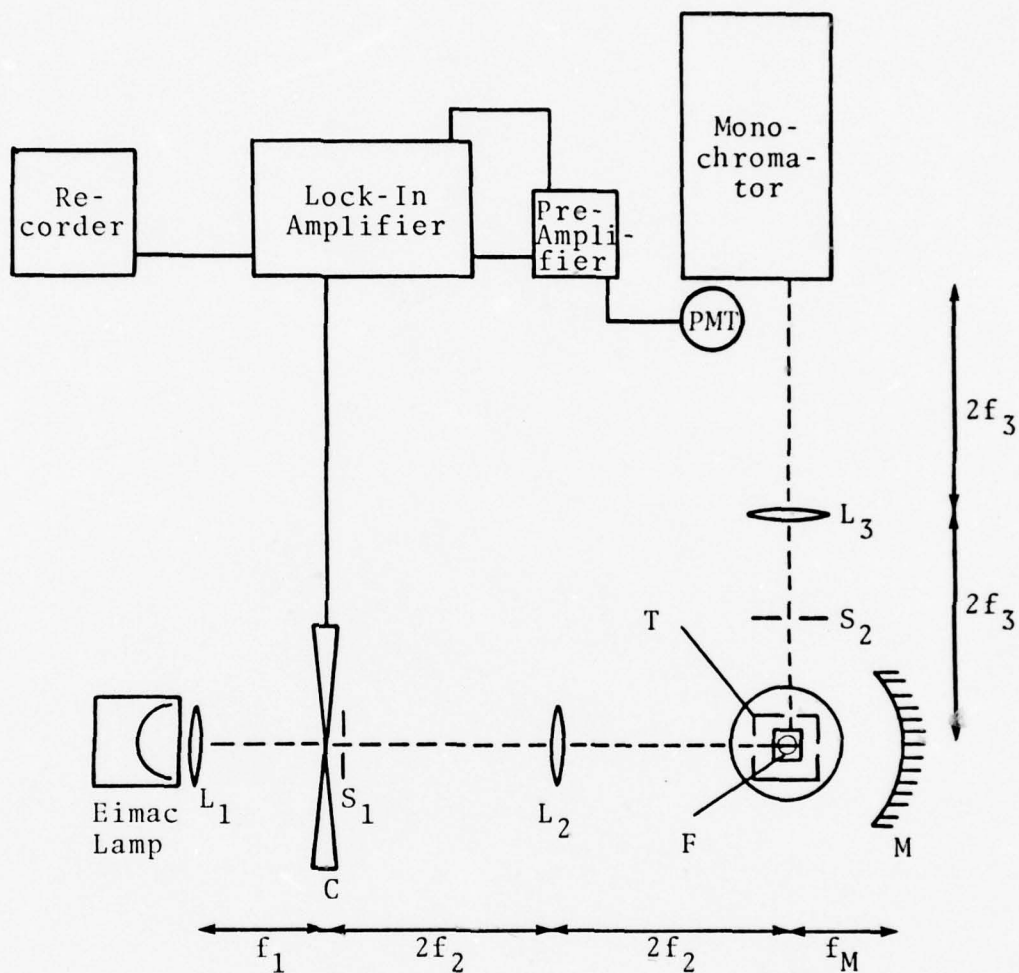


Figure 3. Schematic of system. Lenses L_1 , L_2 , and L_3 focus the illumination and measuring beams. M is a 6-in. spherical mirror. C is the chopper. S_1 and S_2 are light stops with apertures set at 1.0 cm diameter. F is the furnace and T is the light trap. Not shown are the SCR power supply, illuminator power supply, PMT power supply, and the programming unit.

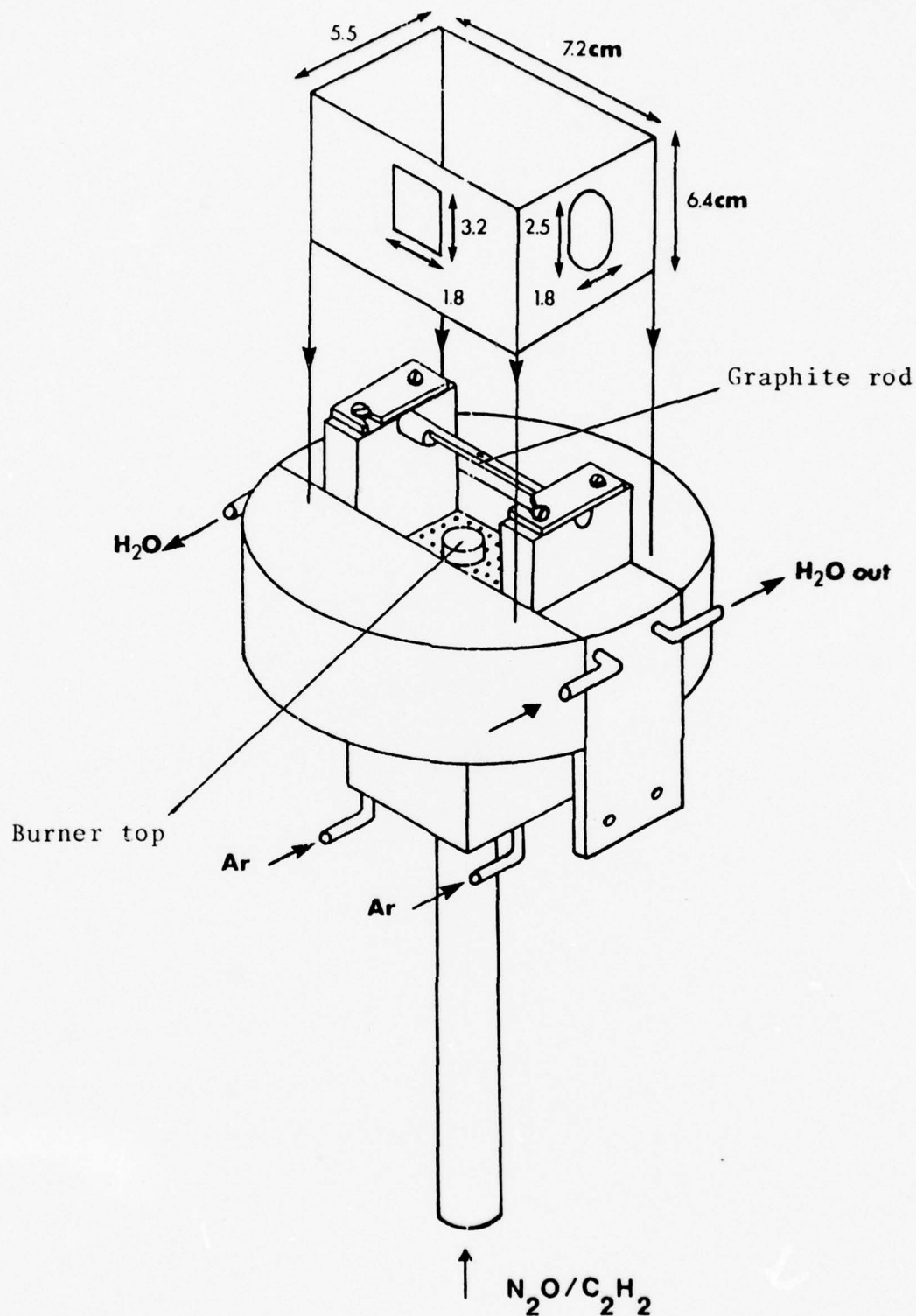


Figure 4. Combination graphite rod-flame atomizer.

Inset into the bottom of the bakelite block was an aluminum block with 56 holes 1.3 mm in diameter to maintain an argon sheath. A circular burner, consisting of 83 capillary tubes 1.0 mm inside diameter and 3.8 cm long, supported a N_2O/C_2H_2 flame above and around the rod.

A removable light trap surrounded the copper blocks and graphite rod. The light trap was a sheet metal box approximately 5.5 cm by 7.2 cm by 6.4 cm high with 2 cm by 3 cm openings cut on three sides for the excitation and measurement beams. The inside of the trap was painted a nonreflective black.

Graphite rods 50 mm long and 6.15 mm in diameter were machined to leave a center section 25 mm long, 2.5 mm high, and 2.5 mm wide. Reproducible sample location on the rod was achieved by drilling a cavity on top of the rod. A He-Ne laser beam was used to align this cavity 4 mm below the intersection of the excitation and measurement beams.

The entire assembly was mounted on a Perkin-Elmer chamber nebulizer system (Perkin-Elmer Corp., model 303-0352, Norwalk, CT 06856) that had the drain and intake clamped closed.

A locally-constructed programming and timing unit (28) was used to establish gas flow sequences as well as the durations and temperatures for the dry, ash, and atomization cycles of the furnace. A schematic diagram of the circuit for the programming unit and a description of its operation is given in Appendix A. The programming unit controls the

amount of current supplied to the furnace to heat the graphite rod.

A photomultiplier detector was mounted at the exit of a 0.5 m Jarrell-Ash monochromator (Jarrell-Ash Co., Newtonville, MA 02160). The wavelength of the monochromator was set at the center of the desired fluorescence line by using an appropriate hollow cathode lamp; a nanoammeter was used to detect the photocurrent. The monochromator was scanned until the nanoammeter showed a maximum output for the desired spectral line.

All analytical measurements were performed with a lock-in amplifier detection system. The photomultiplier output was amplified by a variable gain preamplifier (Ithaco, model 164, Ithaca, NY 14850) prior to detection by a lock-in amplifier (Ithaco Dynatrac 391, Ithaca, NY 14850) referenced to the Eimac source chopped at 250 Hz (Princeton Applied Research, model 125, Princeton, NJ 08540). The amplifier output was recorded by a chart recorder (Linear Instruments Corp., model 261, Costa Mesa, CA 92626) from which the signal peak height (mv) was measured.

Experimental Procedures

The programming unit was calibrated for graphite rod temperature by using a W-W/Re thermocouple probe to determine the temperature of the rod at various settings of the programming potentiometers. The resulting data were used to

construct curves of temperature versus potentiometer settings. The curves were used to set an approximate temperature for the graphite rod for the dry, ash, and atomization cycles (see Appendix B) by setting the potentiometers on the programming unit.

Gas flows were measured by rotameters calibrated in 1 min^{-1} using a mass flow meter (Teledyne Hastings-Raydist, Hampton, VA 23661) and a digital voltmeter. Stock 1000 ppm aqueous standard solutions were prepared from reagent-grade materials according to the procedures outlined by Smith and Parsons (29). These stock solutions were used to prepare 1, 5, 10, 25, 50, 100, and 500 ppm solutions. The oil standards were the Special Spectrometric Calibration Standards obtained from the Naval Air Rework Facility, Naval Air Station, Pensacola, FL. These standards contained the elements Al, Cr, Cu, Fe, Pb, Mg, Ni, Si, Ag, Mo, Sn, and Ti at concentrations of 0, 3, 10, 30, 50, and 100 ppm. Synthetic and real correlation oil samples from the Naval Air Rework Facility were analyzed for the metals of interest.

According to Parson et al. (30), atomic fluorescence intensity is dependent on the following parameters:

1. oxidant gas flow rate,
2. fuel to oxidant ratio,
3. sheath gas flow rate,
4. height of measurement above graphite rod,
5. slit width.

In addition, the graphite rod variables include the time for each cycle, which depend in a complex manner on each sample matrix, as well as the temperature for each cycle. Because very low limits of detection were not a requirement for this study, no attempt was made to maximize all parameters.

In order to minimize formation of analyte oxides, the $\text{N}_2\text{O}/\text{C}_2\text{H}_2$ flame is adjusted to a "red feather" (31) resulting in flow rates of 7.2 l min^{-1} for N_2O and 4.3 l min^{-1} for C_2H_2 . An aqueous aluminum standard solution was used to optimize sheath gas flow rate and slit width. The values giving the best signal-to-background were an argon flow of 2.4 l min^{-1} and slit width $350 \text{ }\mu\text{m}$ (see Appendix C).

One- μl samples were introduced onto the graphite rod using a Micropettor A syringe (Scientific Manufacturing Industries, Emeryville, CA 94608) using disposable capillary tubes. One series of standard and unknown samples were determined rapidly on a single graphite rod in order to minimize the effects of aging of the graphite rod.

For aqueous solutions, optimum graphite rod conditions were dry cycle temperature of 120°C for 10 s, ash cycle temperature of 400°C for 5 s, and atomization cycle time of 3 s (the graphite rod wall temperature was about 2700°C as determined by an optical pyrometer).

For oil samples, the dry cycle was eliminated. The ash temperature was increased to 550°C for 7 to 9 s to allow the dissipation of smoke from the oil ignition. The atomization

time and temperature remained the same as for the aqueous samples.

The gas flow sequence for all samples is given in Table 1.

Table 1. Gas flow sequence.

Cycle	Gas			
	air	N_2O	C_2H_2	Ar
dry	ON	OFF	OFF	ON
ash	OFF	ON	OFF	ON
atomization	OFF	ON	ON	ON
cool	ON	OFF	ON	ON

RESULTS

Chromium (359.3 nm), aluminum (396.1 nm), and molybdenum (313.2 nm) were measured in aqueous and oil standard solutions. The elements were then determined in synthetic and real jet engine lubricating oil samples using calibration curves obtained at the same time as the samples. The oil samples were paired correlation samples* of the Interservice Oil Analysis Program and were provided by the Naval Air Rework Facility, Naval Air Station, Pensacola, FL. The samples included a pair of synthetic samples and a pair of real samples. The experimental conditions are given below in Table 2.

* Each correlation sample set consists of 4 individual samples. Two samples are synthetic samples known to contain the elements of interest. The other two samples are real samples taken from aircraft engines, and these two samples may or may not contain the elements of interest.

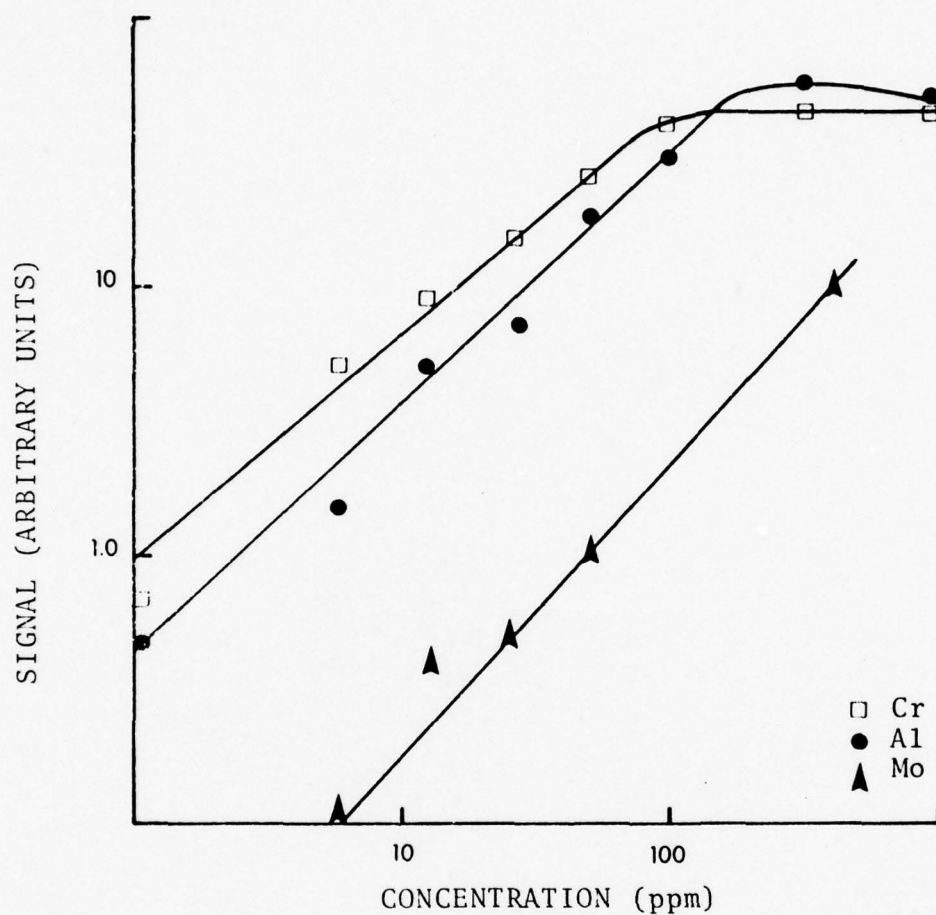


Figure 5. Analytical calibration curves for Cr, Al, and Mo in aqueous standards.

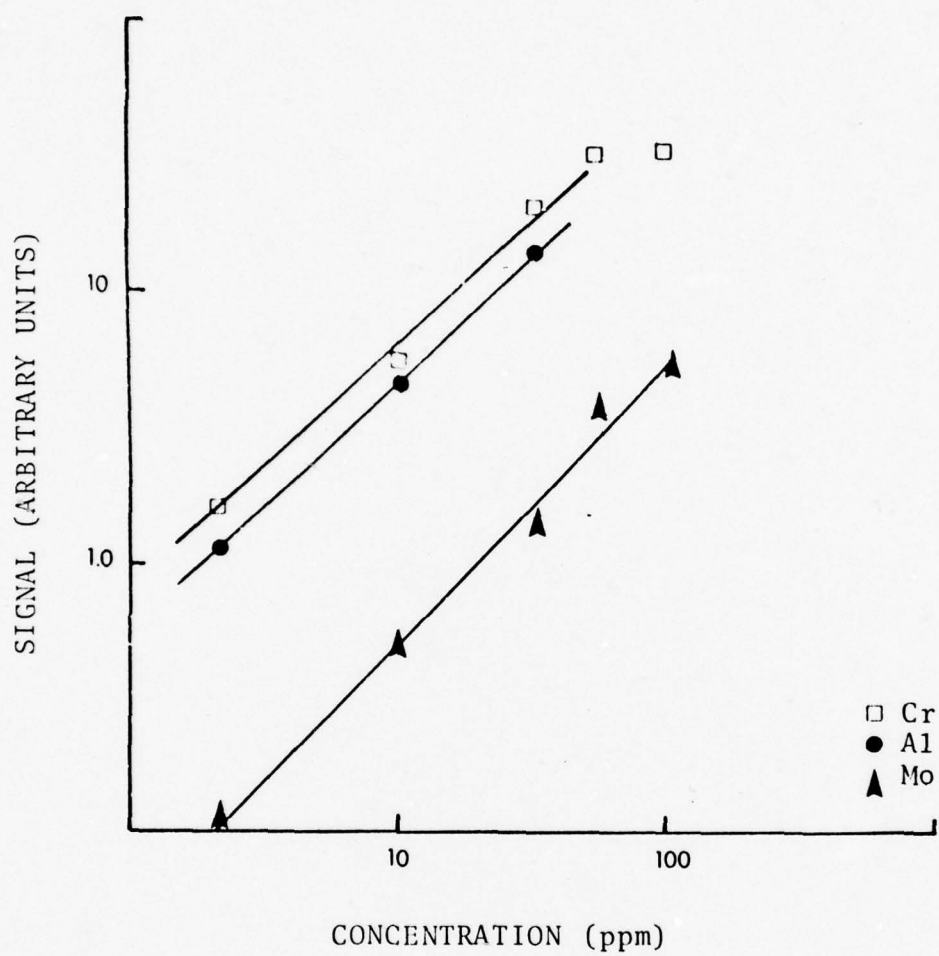


Figure 6. Analytical calibration curves for Cr, Al, and Mo in oil standards.

Table 2. Experimental conditions.

Gas flow rates	
N ₂ O ₂	7.2 l min ⁻¹
C ₂ H ₂	4.3 l min ⁻¹
Ar	2.4 l min ⁻¹
Time constant	40 ms
PMT voltage	-700 V
Illuminator power supply	20 A
Monochromator	
slit width	350 μ m (10 Å bandpass)
slit height	5 mm
Chopper	250 Hz

The results of the oil analyses are given in Table 3. These results are evaluated with respect to the accuracy and repeatability criteria of the Interservice Oil Analysis Program (32). The reported mean values of the paired samples are plotted, one on the horizontal axis, the other on the vertical axis (point A in Figure 7). A 45-degree line is drawn through point A. A rectangle is drawn centered around point A such that the ends of the rectangle indicate the accuracy criteria limits measured from point A along the 45-degree line, and the sides of the rectangle indicate the repeatability criteria limits measured from the 45-degree line. The experimental data are plotted for each pair in the same manner as for the reported mean values. Experimental data falling within the rectangle satisfy both the accuracy and repeatability criteria.

Table 3. Results of oil analyses for Cr, Al, and Mo, and relative standard deviations.

Sample	Cr				Al				Mo			
	This Work (ppm)	(RSD) (%)	IOAPA (ppm)	Crit ^b	This Work (ppm)	(RSD) (%)	IOAPA (ppm)	Crit ^b	This Work (ppm)	(RSD) (%)	IOAPA (ppm)	Crit ^b
145	13	(44)	27	N	25	(20)	26	Y	16	(32)	30	N
146	13	(8)	24		21	(20)	22		13	(22)	25	
147	6	(5)	3.6	N	2	(6)	3.1	Y	1	(28)	1.4	Y
148	5	(28)	3.0		1	(14)	2.4		1		1.1	
161	11	(13)	11	Y	6	(47)	11	N	23	(28)		
162	9		9.3		9	(19)	9		22	(6)		
163	3	(35)	2.9	Y	3	(23)	2.5	Y	9			
164	3	(62)	2.2		3	(24)	2.0		1			
165	23	(33)	49	N	29	(7)	47	N	12	(18)		
166	20	(43)	43		26	(4)	41		9	(3)		
167	2		2.2	Y	21	(30)	23	Y	2			
168	1		1.7		17		21		2			

^aThe reported values are the mean values from atomic absorption measurements made by 61 laboratories participating in the Oil Analysis Correlation Study of the Interservice Oil Analysis Program.

^bThe symbols in this column indicate if the experimental results satisfy the accuracy and repeatability criteria (Y) or if the results fail the criteria (N).

^cThe values for Mo are from atomic emission measurements. The data were not available for samples 161-168. Where no RSD value is given, there were too few data points to determine a valid value.

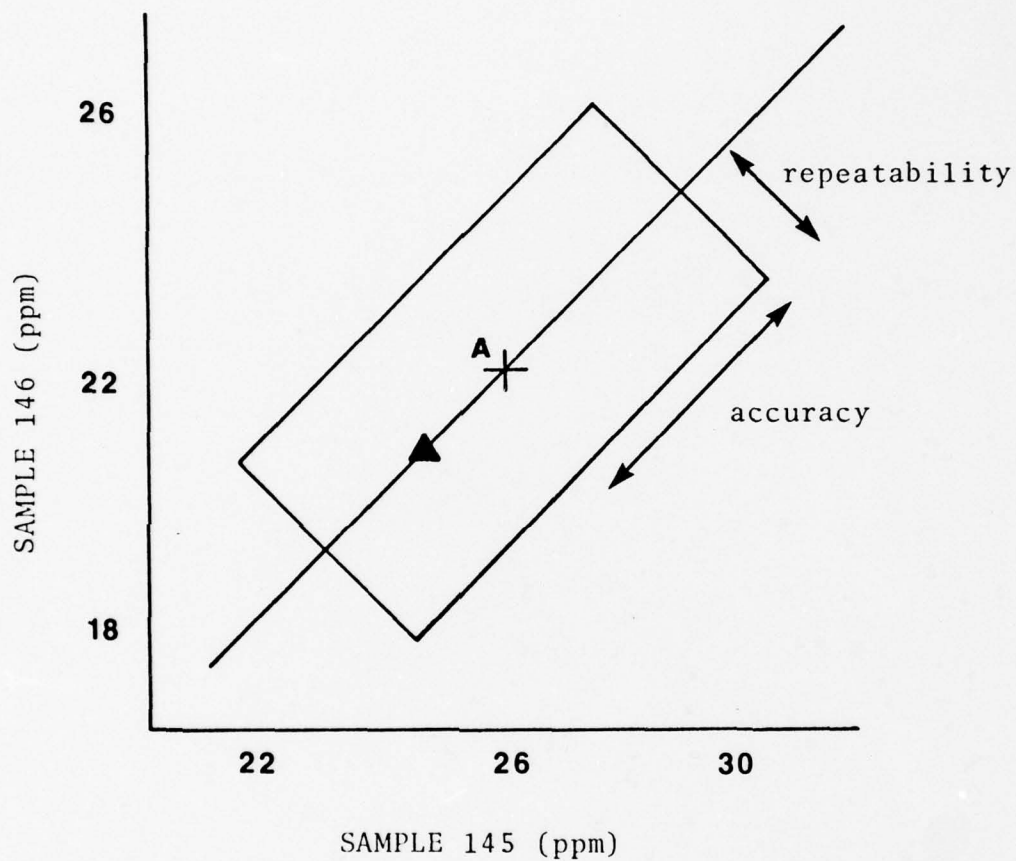


Figure 7. Correlation plot (32) of Al for samples 145 and 146. \blacktriangle indicates the experimental data obtained in this study. Repeatability and accuracy ranges are set by IOAP.

Limits of detection in the oil samples were 0.4 ppm for Cr, 0.3 ppm for Al, and 1.0 ppm for Mo. The linear dynamic range in the oil samples was about 100 ppm for Cr and Al, and slightly less than 500 ppm for Mo.

DISCUSSION

The results obtained in this study compared favorably with the Interlaboratory Correlation results for the real oil samples. Analyses for 6 of 7 real-sample pairs met the military criteria for both accuracy and repeatability. Including the synthetic oil samples, however, only 8 of 14 pairs of determinations were within the criteria. For the sample pairs that failed the criteria, all but one were low. The overall relative standard deviation was about 23%. *2 in probably confirmed by AC*

The described system was simpler and more convenient to operate than standard atomic absorption instruments used for oil analyses. A single excitation source was used for all elements, the samples required no pretreatment, and the system was capable of rapid analysis. For example, 3 sets of samples were analyzed for 2 elements (24 determinations) in 20 to 30 minutes. In addition, the system was capable of detecting and measuring elements such as Al and Mo that are not routinely determined by standard atomic absorption flame methods. Titanium was also detectable with this system, but not at low enough concentrations to perform oil analyses. *that one with AC*
TC must have

The contribution to the error from the detection and measurement system was assumed to be small compared to the total error. The light trap shielded the detector from black

body emission from the heated graphite rod. It was also assumed that the gas composition and flow rates were exactly reproducible and thus remained constant for all measurements.

Sources of errors that must be considered include chemical interferences, errors associated with sampling small volumes, and errors associated with properties of the graphite rod.

Chemical interferences affecting the free-atom fraction, β , include ionization of analyte, compound formation of the analyte with flame gas products or the graphite rod, and solute vaporization interferences.

The extent of ionization depends primarily on the flame gas temperature, the analyte type, and the concentration of free electrons in the flame. The free-atom fraction due only to compound formation is dependent on the flame gas temperature, analyte type, and the concentration of the flame gas products involved in the formation of the compound. Solute vaporization efficiency, ϵ , is affected by flame gas composition and temperature.

The peak concentration, n_p , of analyte in a sample vaporized in a cuvette is proportional to $\epsilon\beta$, the efficiency of producing atoms from the sample. The factor $\epsilon\beta$ should be nearly unity for substances that are completely vaporized within a cuvette, assuming that the atmosphere is inert. In this system, however, the atmosphere is a N_2O/C_2H_2 flame, and in such a flame $\epsilon\beta$ can be orders of magnitude less than unity (33). Compound formation with flame gas products is

not strictly an interference because β should be constant for any given analyte in a given flame (composition and temperature constant).

In Figure 8, it is shown that the input power to the graphite rod (and thus, the temperature) increased as the rod aged. While the current through the rod remained constant (determined by the programming unit), the voltage across the rod (determined by the resistivity of the rod) increased. A total power change of 75% was observed during the useful life of a rod. This resulted in a temperature change of about 500°C or 19%. Reported (34) relationships of the heating rate on peak absorbance vary from linear-to-exponential increases in the signal peak to a decrease in signal peak as the rate of heating increases further.

Uncertainties associated with using small sample sizes arise from the act of withdrawing the test sample from a much larger sample having a complex matrix, and from the reproducible placement of the sample within the atomization cell.

The oil samples were assumed to be homogeneous because no suspended particulate matter was observed. Most samples were clear or only slightly darkened, however, samples 167 and 168 were very black and were more viscous than the other samples. The reproducible placement of the samples was enhanced by using the laser to align the cavity on the graphite rod directly below the measurement cell. Thus, errors due to sample placement were minimized.

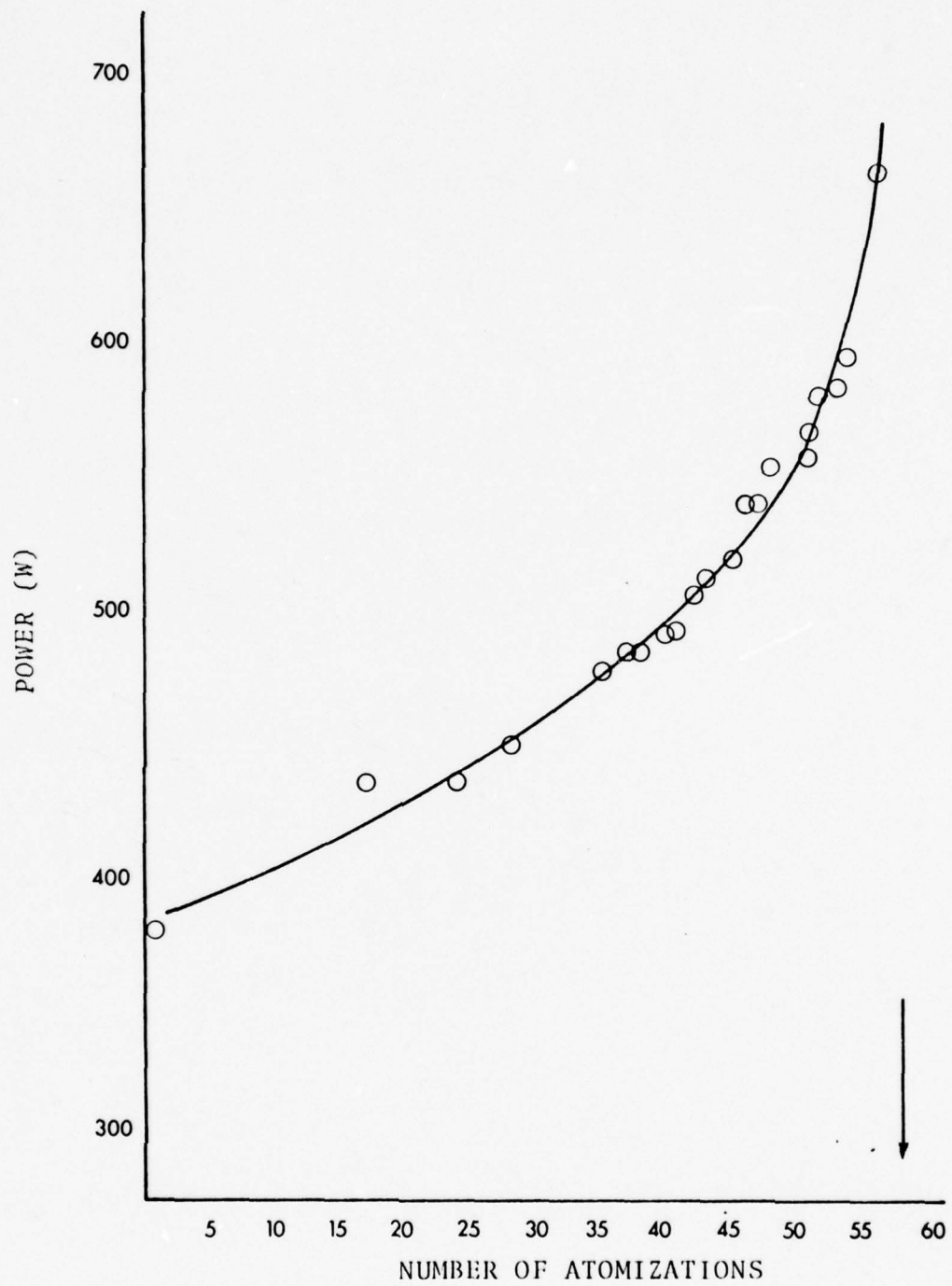


Figure 8. Change in power input as graphite rod aged. The arrow indicates when the rod burned through.

Another major source of uncertainty was associated with the graphite rod furnace atomizer. Syty (35) gave the precision of measurements from a graphite rod as 5% to 8%. Molnar et al. (14) recognized that aging of the rod reduced reproducibility, but they reported that the untreated POCO graphite gave 2% to 4% reproducibility at advanced age (150-200 determinations).

Sturgeon (34) recently discussed the problems associated with electrothermal atomizers for the atomic absorption process. While the primary factors influencing the signal-time characteristics of all elements are the heating rate of the atomizer and its geometry, a third factor that can alter the kinetics of atom formation is the physicochemical nature of the graphite surface (porosity, reactivity, density, permeability). The effects of this third factor are more pronounced with refractory elements such as Mo and Ti.

Factors arising from the physicochemical nature of the graphite surface are complex and were not experimentally measured in this study. Certainly many of the effects are interrelated. For example, as the porosity increases, so would the reactivity due to increased contact between the graphite and the analyte.

While the effects of changes in the physicochemical nature were not directly measured, physical changes in the graphite rod with age were observed. On a new rod, samples formed spherical beads, whereas on an older rod, the samples spread out along the rod. This spreading had the effect of

increasing the path length ℓ . The observed maximum increase was about 3 times ℓ . The luminescence radiance expression includes the path length in the following term:

$$\frac{L\ell\ell'}{2L\ell' + 2\ell\ell' + 2L\ell}$$

The result of the observed increase in ℓ is an increase in B_L by 28%, assuming the concentration of analyte does not change.

A final area of uncertainty concerns post- and prefilter effects on the luminescence radiance (36). The reabsorption in the cell volume of luminescence of an analyte species that is not being illuminated by excitation radiation decreases the luminescence radiance by the factor f_I (postfilter effect). For low concentrations of analyte, $f_I = 1$, but for high concentrations of analyte (for transitions terminating in ground or near ground states and for the right angle illumination measurement case), f_I is given by

$$f_I = \sqrt{1 + \Delta L/L} - \sqrt{\Delta L/L}$$

where ΔL is the thickness of the sample nearest the detector and not being excited and L is the sample path length being excited. As $\Delta L/L$ becomes very large (less and less sample is being excited), f_I approaches zero, and as $\Delta L/L$ approaches zero (more and more sample is being excited), f_I approaches unity.

The luminescence radiance is decreased by a factor f_E for the right angle case if the luminescence in the portion of the cell nearest the source is not measured (prefilter

effect). For atomic fluorescence excited by a continuum source and for high concentration of analyte,

$$f_E = \sqrt{1 + \Delta l / l} - \sqrt{\Delta l / l}$$

where Δl is the cell length over which atomic fluorescence is not measured and l is the cell length over which atomic fluorescence is measured. As $\Delta l / l$ becomes very large, f_E approaches zero and as $\Delta l / l$ becomes very small, f_E approaches unity. The increase in l observed in this system could result in a f_E of less than unity with a corresponding decrease in the measured luminescence.

In summary, the major source of error was associated with the aging of the graphite rod. The effects are complex and sometimes opposite in direction of error. Increasing path length increases the volume term in the luminescence expression, but it also contributes to a prefilter factor that decreases the measured luminescence. The increasing temperature affects the factor $\epsilon\beta$, but according to Sturgeon (34), the effect of increasing temperature is first an increase in peak absorbance and then a decrease in peak absorbance.

CONCLUSIONS

This system demonstrated potential as a simple, rapid, and convenient method to analyze small samples having complex matrices. It was particularly promising for elements such as Al and Mo that are not routinely analyzed in oil samples by atomic absorption methods.

There was a large uncertainty in the system as evidenced by the range in RSD of 3-62%. The major source of uncertainty was due to the rapid aging of the electrically-heated graphite rod in the N_2O/C_2H_2 flame. An immediate improvement should be realized by the use of pyrolytic graphite or pyrolyzed POCO graphite in place of the untreated graphite.

The system was successful in determining Cr, Al, and Mo in real jet engine lubricating oils. Limits of detection for Cr, Al, and Mo were 0.4, 0.3, and 1.0 ppm, respectively.

APPENDIX A
CURRENT CONTROL/TIMING CIRCUIT (28)

The current control/timing circuit consisted of a timing and control circuit and a current adjusting switching circuit. Basically, μA 741's were used as voltage comparators between a reference voltage (summations of V_1 , V_2 , V_3 , V_4 , and V_5) and a time variable voltage, V_t , where V_2 , V_3 , V_4 , and V_5 were the basis for variable time durations in the drying, ashing, atomizing, and cooling cycles, respectively. Voltage V_1 gave a present delay period between starting and drying. Voltage V_i was internally set to give integration of V_i to V_t at a ramp of about 100 mV s^{-1} .

Before the start button was pushed, the following conditions held:

1. $V_t < V_1, V_2, V_3, V_4, V_5$;
2. operational amplifiers A, C, E, F, and H outputs were negative, therefore $Q_1, Q_3, Q_5, Q_8, Q_9, Q_{11}$, and Q_7 were all turned off;
3. operational amplifiers B, D, and G outputs were positive so Q_2, Q_4, Q_6 , and Q_{10} were all turned off;
4. K_1 through K_6 were all off.

When the start button, S_2 , was pushed, Q_7 was shorted out, turning on relay K_4 and LED D_{21} . When K_4 turned on,

+20 V was supplied to bias Q_7 thus keeping K_4 on as well as D_{21} . When K_4 was turned on, OA1 started integrating V_i , thus building up V_t . When K_4 turned on, then I_{sensIN} was switched to be controlled by K_1 , K_2 , and K_3 . At this point, K_4 switched I_{sensIN} to K_1 , which is off, and shorted I_{sensIN} to $I_{sensOUT}$.

When $V_t > V_1$, then A's output went positive, Q_1 was turned on (Q_2 was previously on) thus turning on K_1 and LED D_{18} . When K_1 turned on, then I_{sensIN} was passed through P_8 to $I_{sensOUT}$ (P_8 controlled the current output of the SCR power supply at that time). *Drying was started.*

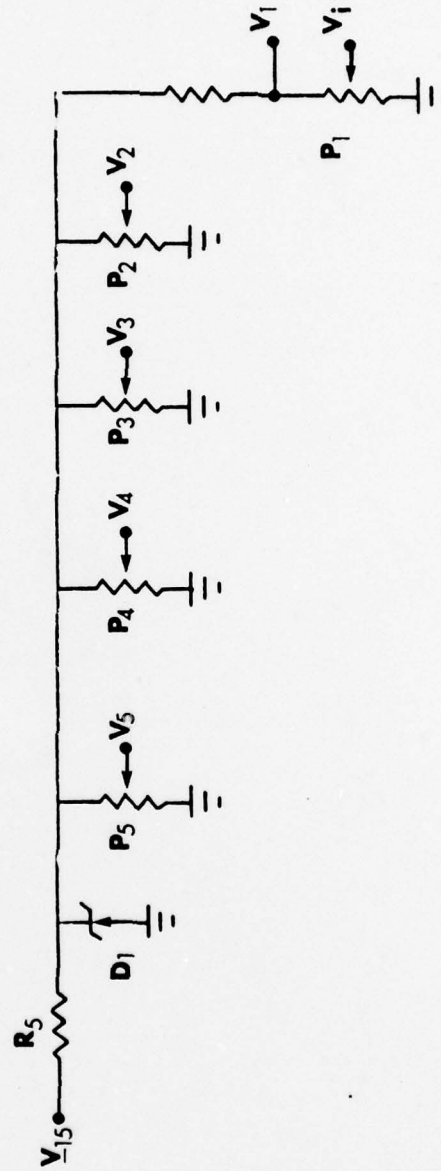
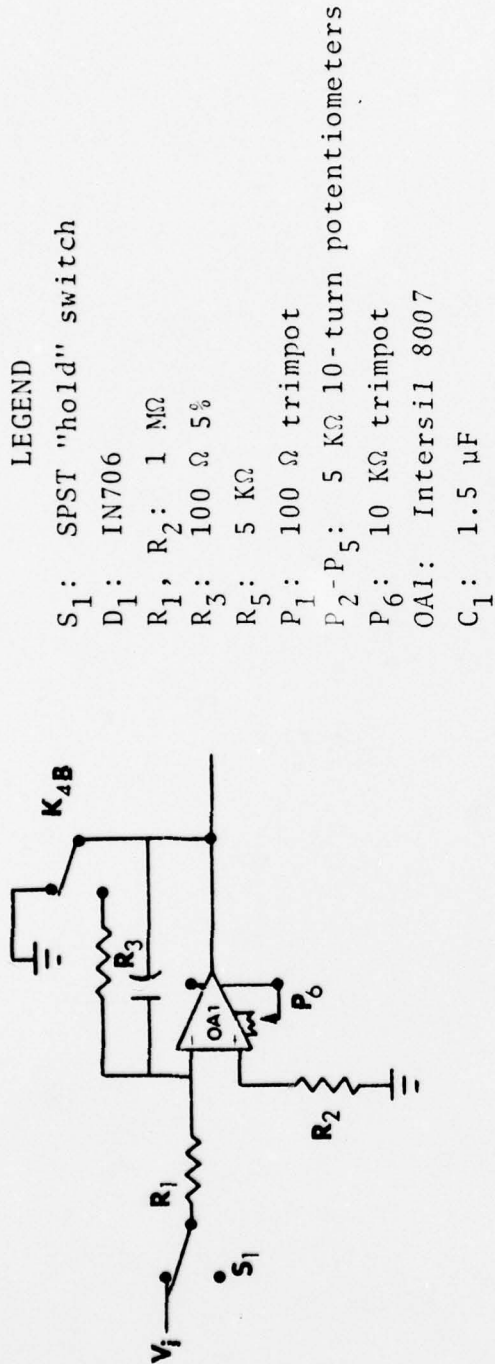
When $V_t > V_1 + V_2$, then C's output went positive. This drove B's output negative, turning off Q_2 (thereby K_1). Since Q_4 and Q_{10} were previously on, when C went positive, Q_3 and Q_9 turned on, turning on K_2 and K_5 . Relay K_5 turned on the solenoid which switched from air to N_2O . When K_2 was on, LED D_{19} was on and control of I_{sensIN} passed through P_9 to $I_{sensOUT}$. *Drying was thereby stopped and ashing started.*

When $V_t > V_1 + V_2 + V_3$, then E's output went positive and D's went negative. Thus, Q_4 went off as did K_2 and D_{19} . At the same time, Q_5 and Q_{11} came on, and since Q_6 was on, K_3 and K_6 came on as well as LED D_{20} . When K_3 was switched on, then I_{sensIN} passed through P_{10} to $I_{sensOUT}$. A solenoid was thrown when K_6 was on, turning on C_2H_2 . *Ashing was therefore stopped and atomization started.*

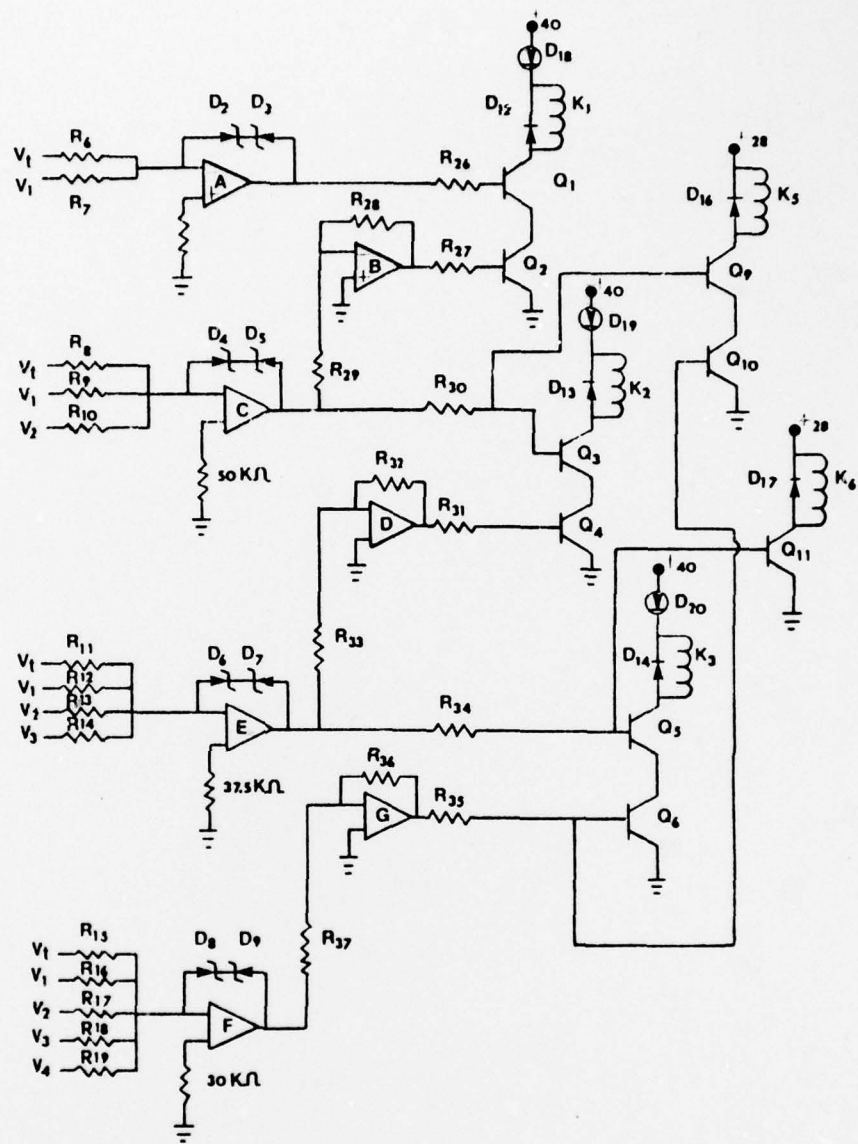
When $V_t > V_1 + V_2 + V_3 + V_4$, F's output went positive. Therefore, G's output went negative, turning off Q_6 and Q_{10} .

When Q_{10} went off, then K_3 went off and I_{sensIN} was then turned to K_1 's normally closed position, shorting I_{sensIN} to $I_{sensOUT}$. When Q_{10} was turned off, so was K_5 . This turned off the solenoid, switching N_2O back to air. *Thus, atomization ended and cooling began.*

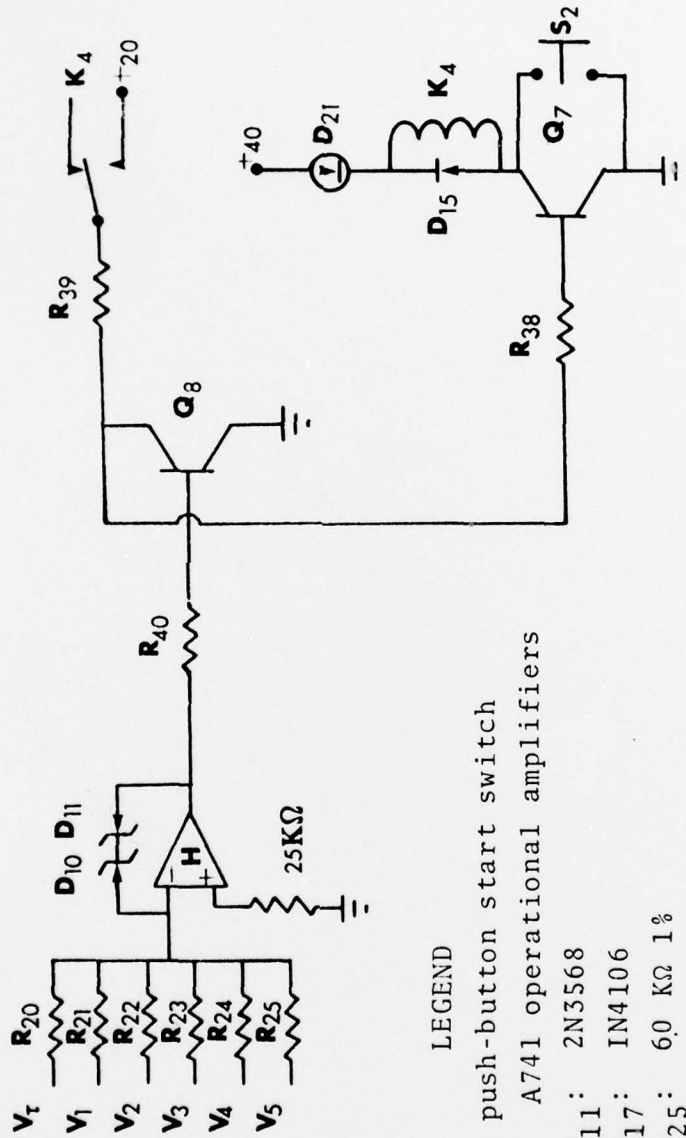
When $V_t > V_1 + V_2 + V_3 + V_4 + V_5$, then H's output went positive, turning on Q_8 . This shorted the +20 V, keeping Q_7 on to ground, thus turning off Q_7 and K_4 . When K_4 was off, then V_t went to zero thereby placing all components at their original status. Since E's output was now negative, Q_{11} was turned off. Therefore, K_6 was off and the solenoid switched back, turning off the C_2H_2 . *Thus, cooling was over and all components were ready for a new cycle.*



REFERENCE AND TIMING VOLTAGES



TIMING AND CONTROL CIRCUIT



LEGEND

S_2 : push-button start switch

A-H: A741 operational amplifiers

Q_1 - Q_{11} : 2N3568

D_2 - D_{17} : IN4106

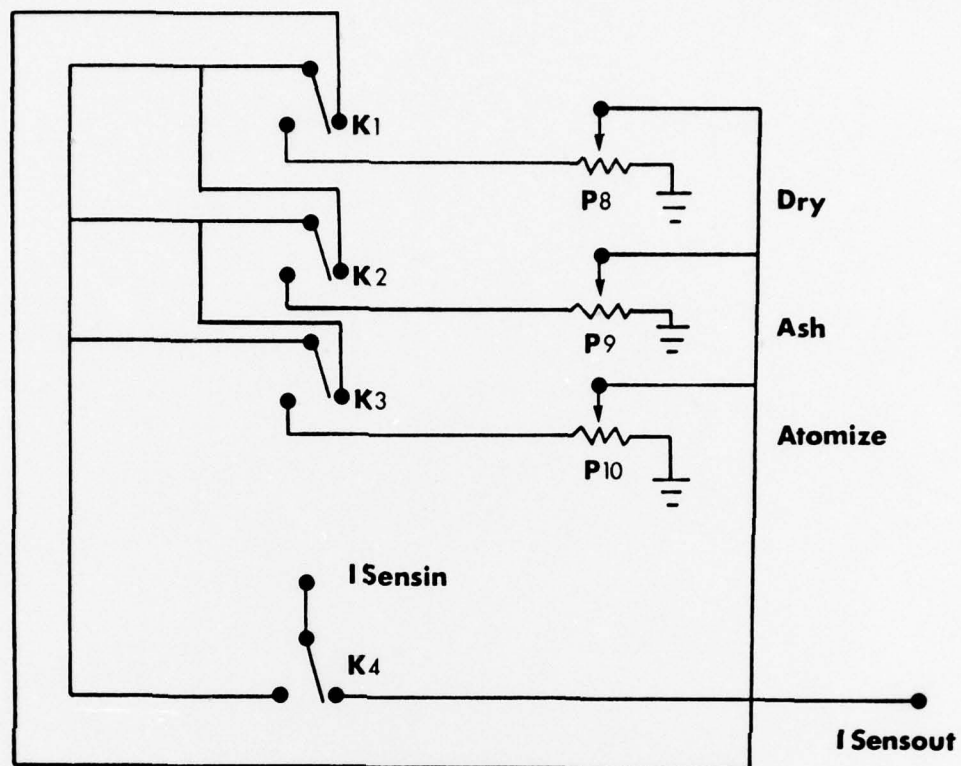
R_6 - R_{25} : 60 $K\Omega$ 1%

R_{26} - R_{40} : 9.1 $K\Omega$ 5%

K_1 - K_4 : 40 vDC relays

K_5 , K_6 : 28 vDC relays

TIMING AND CONTROL CIRCUIT (continued)



LEGEND

K₁-K₄: 40 vDC relays

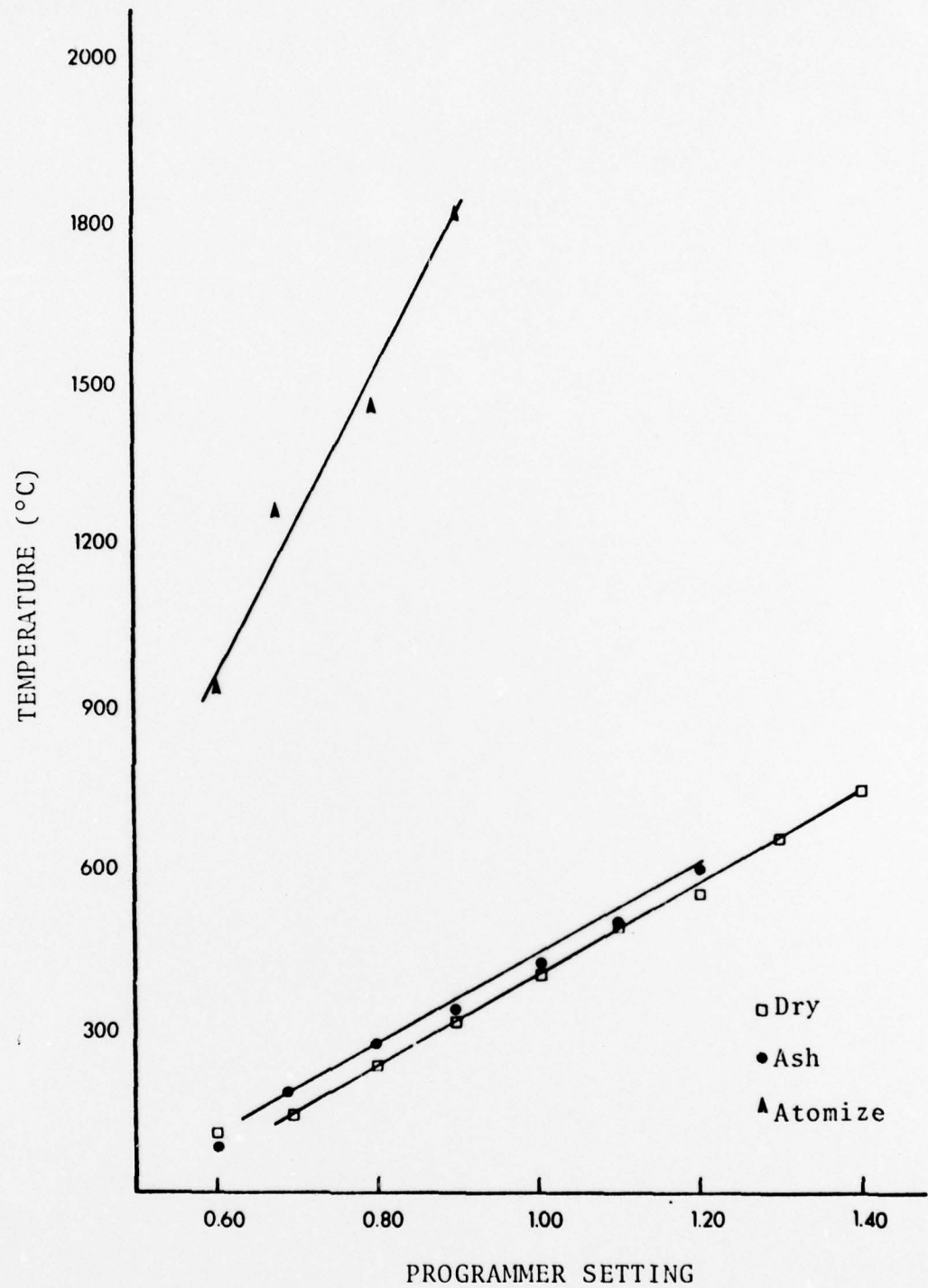
P₈-P₁₀: 200 Ω 10-turn potentiometers

CURRENT ADJUSTING SWITCHING CIRCUIT

APPENDIX B
TEMPERATURE CALIBRATION DATA

Cycle	Potentiometer Setting	Power Supply Voltage (V)	Current (A)	Temperature* (°C)
dry	0.60	1.2	10	110
	0.70	1.6	12	182
	0.80	1.8	15	271
	0.90	2.0	20	327
	1.00	2.2	22	416
	1.10	2.4	25	488
	1.20	2.6	29	593
ash	0.60	1.2	10	143
	0.70	1.6	13	160
	0.80	1.8	16	227
	0.90	2.1	20	321
	1.00	2.3	23	399
	1.10	2.4	25	488
	1.20	2.7	30	538
	1.30	2.8	32	660
	1.40	2.9	36	754
	1.50	3.1	40	871
atomization	0.60	3.2	40	954
	0.70	3.7	49	1282
	0.80	4.6	53	1460
	0.90	5.8	56	1816

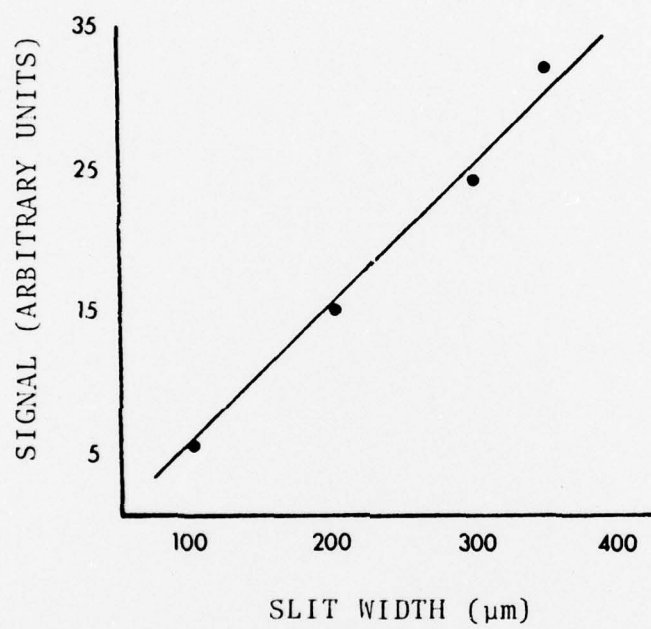
* Data obtained by placing a thermocouple probe in the cavity of the graphite rod until a steady reading was read on a millivolt meter. The thermocouple was a W-W/Re type.

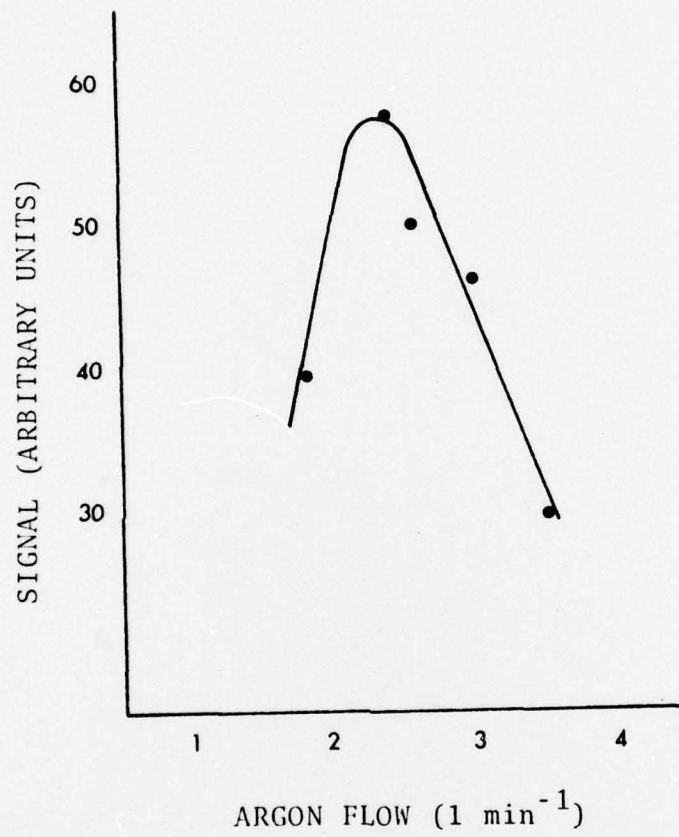


TEMPERATURE CALIBRATION CURVES

APPENDIX C

SLIT WIDTH AND ARGON FLOW OPTIMIZATION





LIST OF REFERENCES

1. R.D. Reeves, C.J. Molnar, M.T. Glenn, J.R. Ahlstrom, and J.D. Winefordner, Anal. Chem., 44, 2205 (1972).
2. J.D. Winefordner and T.J. Vickers, Anal. Chem., 36, 161 (1964).
3. J.D. Winefordner and R.A. Staab, Anal. Chem., 36, 1165 (1964).
4. T.S. West, Analyst, 91, 69 (1966).
5. R.M. Dagnall, T.S. West, and P. Young, Talanta, 13, 803 (1966).
6. R.F. Browner, Analyst, 99, 617 (1974).
7. D.G. Mitchell, and A. Johansson, Spectrochim. Acta, 25B, 175 (1970).
8. R. Smith, D.M. Stafford, and J.D. Winefordner, Appl. Spectrosc., 25, 477 (1969).
9. R.L. Miller, L.M. Fraser, and J.D. Winefordner, Can. Spectrosc., 14, 2 (1969).
10. J.D. Winefordner, V. Svoboda, and L.J. Cline, CRC Crit. Rev. Anal. Chem., 1, 233 (1970).
11. D.J. Johnson, F.W. Plankey, and J.D. Winefordner, Anal. Chem., 46, 1898 (1974).
12. D.J. Johnson, F.W. Plankey, and J.D. Winefordner, Can. J. Spectrosc., 19, 151 (1974).
13. D.J. Johnson, F.W. Plankey, and J.D. Winefordner, Anal. Chem., 47, 1739 (1975).
14. C.J. Molnar, R.D. Reeves, M.T. Glenn, J.R. Ahlstrom, J. Savory, and J.D. Winefordner, Appl. Spectrosc., 26, 606 (1972).
15. R.D. Reeves, C.J. Molnar, M.T. Glenn, J.R. Ahlstrom, and J.D. Winefordner, Anal. Chem., 44, 2205 (1972).

16. K.G. Brodie and J.P. Matousek, Anal. Chem., 43, 1557 (1971).
17. J.F. Alder and T.S. West, Anal. Chim. Acta, 58, 331 (1972).
18. S. Omang, Anal. Chim. Acta, 56, 470 (1971).
19. R.D. Reeves, C.J. Molnar, and J.D. Winefordner, Anal. Chem., 44, 913 (1973).
20. B.M. Patel, R.D. Reeves, R.F. Browner, C.J. Molnar, and J.D. Winefordner, Appl. Spectrosc., 27, 171 (1973).
21. D.A. Katskov, L.P. Kruglikova, and B.V. L'vov, Anal. Abstr., 30, 3J59 (1976).
22. V.A. Razumov, Anal. Abstr., 33, 3J66 (1977).
23. J.D. Winefordner, S.G. Schulman, and T.C. O'Haver, Luminescence Spectrometry in Analytical Chemistry, John Wiley and Sons, New York (1972), pp. 81-94.
24. J.D. Winefordner, V. Svoboda, and L.J. Cline, CRC Crit. Rev. Anal. Chem., 1, 233 (1970).
25. J.D. Winefordner, S.G. Schulman, and T.C. O'Haver, Luminescence Spectrometry in Analytical Chemistry, John Wiley and Sons, New York (1972), p. 82.
26. Ibid., p. 100.
27. F.S. Chuang and J.D. Winefordner, Appl. Spectrosc., 29, 412 (1975).
28. L.P. Hart, designer, J.D. Bradshaw, unpublished manuscript, Dept. of Chem., Univ. of Florida, May 14, 1977.
29. B.W. Smith and M.L. Parsons, J. Chem. Ed., 50, 680 (1973).
30. M.L. Parsons, B.W. Smith, and G.E. Bentley, Handbook of Flame Spectroscopy, Plenum Press, New York (1975), pp. 24-26.
31. J.D. Winefordner, S.G. Schulman, and T.C. O'Haver, Luminescence Spectrometry in Analytical Chemistry, John Wiley and Sons, New York (1972), p. 127.
32. Interservice Oil Analysis Program, undated letter, Naval Air Rework Facility, Naval Air Station, Pensacola, Florida.

33. J.D. Winefordner, S.G. Schulman, and T.C. O'Haver, Luminescence Spectrometry in Analytical Chemistry, John Wiley and Sons, New York (1972), p. 129.
34. R.E. Sturgeon, Anal. Chem., 49, 1255A (1977).
35. A. Syty, CRC Crit. Rev. Anal. Chem., 4, 155 (1974).
36. J.D. Winefordner, S.G. Schulman, and T.C. O'Haver, Luminescence Spectrometry in Analytical Chemistry, John Wiley and Sons, New York (1972), pp. 95-96.

BIOGRAPHICAL SKETCH

Robert L. Vaughn was born February 4, 1947, in Anniston, Alabama. He graduated from Saks High School there in 1965, and attended nearby Jacksonville State University for one year prior to accepting an appointment to the United States Air Force Academy near Colorado Springs, Colorado.

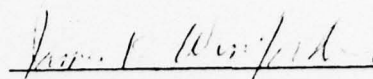
At the Air Force Academy, he was twice named to the Dean's List. He graduated in 1970 with a Bachelor of Science degree in chemistry.

He completed USAF Undergraduate Pilot Training in 1971, and piloted B-52 bombers until May 1976, when he was selected by the Air Force Institute of Technology for graduate study in analytical chemistry. Upon completion of his studies he will be assigned to the Frank J. Seiler Research Laboratory, USAF Academy, Colorado.

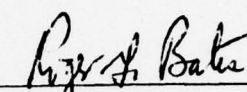
Robert L. Vaughn is a member of the American Chemical Society and the Analytical Division.

He is married to the former Jo Anne Linder, and they have two children.

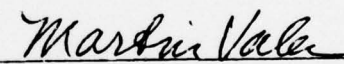
I certify that I have read this study and that in my opinion it conforms to acceptable standards of scholarly presentation and is fully adequate, in scope and quality, as a thesis for the degree of Master of Science.


James D. Winefordner, Chairman
Graduate Research Professor
of Chemistry

I certify that I have read this study and that in my opinion it conforms to acceptable standards of scholarly presentation and is fully adequate, in scope and quality, as a thesis for the degree of Master of Science.


Roger G. Bates
Professor of Chemistry

I certify that I have read this study and that in my opinion it conforms to acceptable standards of scholarly presentation and is fully adequate, in scope and quality, as a thesis for the degree of Master of Science.


Martin T. Vala
Associate Professor of Chemistry

This thesis was submitted to the Graduate Faculty of the Department of Chemistry in the College of Arts and Sciences and to the Graduate Council, and was accepted as partial fulfillment of the requirements for the degree of Master of Science.

March, 1978

Dean, Graduate School